View Article Online / Journal Homepage / Table of Contents for this issue

"Smart dust": nanostructured devices in a grain of sand

Michael J. Sailor and Jamie R. Link

Received (in Cambridge, UK) 18th November 2004, Accepted 20th January 2005
First published as an Advance Article on the web 10th February 2005
DOI: 10.1039/b417554a

Published on 10 February 2005. Downloaded by Open University on 07/07/2013 20:44:05.

The term "smart dust" originally referred to miniature wireless semiconductor devices made using fabrication techniques derived from the microelectronics industry. These devices incorporate sensing, computing and communications in a centimetre-sized package. This article discusses the construction of much smaller silicon-based systems, using the tools of nanotechnology. The synthesis of millimetre- to micron-sized functional photonic crystals made from porous silicon is described. It is shown how the various optical, chemical, and mechanical properties can be harnessed to perform sensing, signal processing, communication and motive functions.

Sensing, computing, communication … and mobility

Kristofer Pister, a professor of electrical engineering at the University of California, Berkeley and one of the pioneers in the wireless sensor networks field, first coined the term "smart dust" in 1997.[1] Extrapolating the recent advances in microelectronics and in wireless communications, he reasoned that a low-power computer could be built within a cubic millimetre of silicon. This "cubic millimetre mote" would contain a battery, a two-way radio, digital logic circuitry, and the capability to monitor its surroundings. Mass-producing the devices using conventional silicon fabrication techniques would make them cheap enough to be disposable, and many of them could be deployed simultaneously to provide a highly redundant network. Pister envisioned using smart dust networks to invisibly monitor factories, buildings, and public spaces. Potential applications included inventory monitoring, controlling lighting and temperature in individual rooms of a large building, and early detection and tracking of the plume from a chemical or biological terror attack.

Although the devices have not yet hit the millimetre size scale Pister proposed almost ten years ago, many companies now build centimetre-scale hardware for wireless, distributed sensor networks.[2] Indeed, for many of the present applications the microscopic "mote of dust" is too small to be useful. Placing sensor packs along a pipeline to detect a leak or rupture, for instance, can be achieved with a thumb-sized device quite conveniently.[3] However, the need to decrease network granularity, reduce cost, lower power consumption and improve reliability of sensor nets is driving the size of the motes down. If a sophisticated device really could be placed in a speck of dust, many additional application areas open up. A speck of dust can go to places that a macroscopic device cannot: a thumb-sized device in a metre-wide pipe can detect a leak; a dust-sized device in a blood vessel may be able to locate a cancerous tumor.

The larger of the "smart dust" devices are constructed using the tools of conventional microelectronics fabrication facilities. These devices are active, containing on-board power sources to run digital circuits and wireless transmitters. In contrast, most

Michael J. Sailor

Professor Sailor received a BS in chemistry from Harvey Mudd College and a PhD in inorganic chemistry from Northwestern University in 1988. He held postdoctoral appointments at Stanford University and The California Institute of Technology before joining the University of California, San Diego in 1990; he became Associate Professor in 1994 and Full Professor in 1996.

Professor Sailor's research focuses on the chemistry, electrochemistry, and photophysics of nanophase semiconductors, with emphasis on photonic crystals, quantum dots and wires, and biocompatible materials. Studies of these materials emphasize applications in medical diagnostics, high-throughput screening, and low-power sensing of toxins, pollutants, and chemical or biological warfare agents.

Jamie R. Link

Jamie R. Link received a BA in Chemistry from Princeton University in 2000. She is currently a PhD student at the University of California, San Diego. She shared the 2002 "The Best of What's New" general technology award from Popular Science Magazine for her "smart dust" photonic crystal sensor work, and received the $50 000 grand prize in the 2003 Collegiate Inventor's Competition for her development of self-assembling "smart dust". In 2004, she was named one of MIT Technology Review Magazine's "Top 100" innovators, the youngest person to receive the distinction that year.

This journal is © The Royal Society of Chemistry 2005

Published on 10 February 2005. Downloaded by Open University on 07/07/2013 20:44:05.

artificial nanomachines are passive devices that function without built-in power. It is difficult to provide power to a nanomachine, and while a number of micro-power sources exist for millimetre scale devices, power remains a limiting factor in this size regime as well. Although solutions will differ for active and passive devices, a common goal for nanotechnology is to minimize or eliminate power requirements while increasing the fidelity of the desired measurement.

The specific challenges can be divided into four areas. Three of the areas are defined along the lines of Pister's originally proposed "sensing, computing, and communication system". The fourth problem, which becomes increasingly difficult with miniaturization, involves movement of the motes: how to place them where you want them when you can't see them. We will call this last area "mobility". This article focuses on passive nanoscale devices, and discusses them in the context of our development of "smart dust"—defined as a sub-millimetre scale device that contains four properties: the ability to position itself, to sense its environment, to perform data or signal processing, and to effect a change in or communicate with the macroscopic world. In short, to move, sense, calculate and respond.

Making dust from porous silicon

Electrochemical etching of silicon wafers is perhaps one of the simplest and cheapest means to build a nanostructure with complex properties. The electrochemical etch produces a porous layer whose thickness, porosity and average pore diameters are precisely controlled. Porous silicon is typically prepared by electrochemically corroding a silicon wafer in an aqueous solution containing hydrofluoric acid and ethanol. The process drills a myriad of nanometre-scale holes along the <100> crystallographic direction in the Si wafer (Fig. 1). By changing the electrochemical current, the electrolyte composition and the dopant characteristics of the wafer, one can tune the average diameter of the pores from a few nanometres to several microns. The cross-sectional image shown in Fig. 1 illustrates how a sudden change in current applied halfway through the etching process results in an abrupt change in average pore diameter.

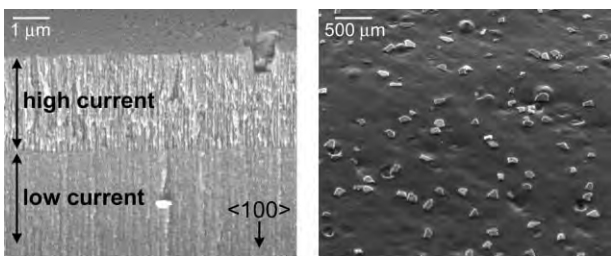

Fig. 1 Producing silicon particles with controlled pore sizes. Left: Cross-sectional SEM image of the porous nanostructure in a porous Si film. The pore size is controlled by the current applied during etching. In this sample, the current was decreased suddenly during preparation, resulting in the abrupt decrease in pore diameter observed. Right: Particles produced by lift-off of the porous film followed by ultrasonic fragmentation. Note the factor of 500 difference in size scale between the two images. Images courtesy of Claudia Pacholski and Yang Yang Li.

The large specific surface area (a few hundred square metres per cubic centimetre, corresponding to about a thousand times the surface area of the polished silicon wafer) makes porous Si a convenient material from which to fabricate many interesting devices: biosensors,[4–10] chemical sensors,[11–20] bioresorbable materials,[21,22] on-chip separators,[23] MEMS power supplies[24–27] and cellular microphysiometers,[28] to name a few. Generation of micron-sized particles from these films is a simple matter of removing the porous Si film from the substrate and fracturing it into pieces. A pulse of current, under the right conditions, is sufficient to undercut the porous Si layer and lift it completely from the Si substrate. These free-standing films are fairly brittle, and they can be fractured into millimetre to micron-sized pieces in an ultrasonic bath (Fig. 1).[29–31]

Photonic crystals—putting the ID tag on a dust particle

Up to this point we have described how to make "dust" of a porous Si nanostructure. Making it "smart" will involve four other aspects—giving it the ability to sense its environment, perform rudimentary signal processing, communicate with the user and move about. The sensing, signal processing and communication aspects all take advantage of the ability to design complex photonic structures in porous Si by manipulating the electrochemical preparation conditions.

Photonic crystals are materials that diffract visible light in a manner similar to how planes of atoms in a crystal diffract X-rays.[32] Two main differences are that the Bragg spacing is on the order of the wavelength of visible, rather than X-ray radiation, and that the refractive index plays a more significant role in determining the Bragg condition for photonic crystals. There are many familiar examples of how Nature uses photonic crystals to make "structural" colors: opals, butterfly wings, the inside of the abalone shell. The shells of many beetles also derive their colors from a photonic crystal, in this case made of multilayers of chitin. The shell of the beetle *Calloodes grayanus*, shown in Fig. 2, is illustrative.

The construction of a photonic crystal by electrochemical etching of Si was first described by Vincent in 1994.[34] The seminal discovery was that porosity, or the amount of silicon

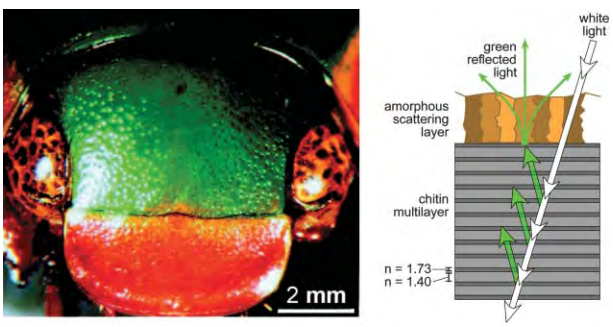

Fig. 2 Photonic crystals in Nature: shell of the beetle *Calloodes grayanus*. Left: Photograph of the beetle, displaying the intense green color of the cuticle. Right: Diagram showing the layered chitin structure that gives rise to the structural color in this organism. Adapted from ref. 33.

 This journal is © The Royal Society of Chemistry 2005

Published on 10 February 2005. Downloaded by Open University on 07/07/2013 20:44:05.

dissolved at the pore–silicon interface at any point in time, directly maps to the current being passed at that instant. Thus if the current density is cycled in real time during the etch, the resulting porous film displays a corresponding modulation in porosity with depth. The variation also represents a modulation in refractive index, and that is the key to construction of photonic structures with porous Si. Just as the alternating optical density of the repeating layers of chitin in the beetle shell diffract and refract light to produce a peak in reflectivity at a precise wavelength, varying the porosity of Si in a porous Si structure produces a similar strong reflection at defined wavelengths.

Vincent's original films consisted of a simple A–B repeat pattern known as a Bragg stack, whose alternating pore morphology is similar to the cross-sectional image shown in Fig. 1. This one-dimensional photonic crystal gave a strong reflection over a relatively broad wavelength range, corresponding to a band of forbidden energies—the photonic bandgap.[32,35,36] Soon afterwards Pavesi, Thönissen, and others showed that more elaborate waveforms can be used in the etch, resulting in dielectric mirrors (quarter-wave Bragg stacks), rugate filters, microcavities, and other advanced optical structures.[14,34,37–43]

Berger *et al.* were the first to add two sine waves together and etch the resulting waveform into silicon. This produced a material whose spectrum displayed characteristics of both component sine waves.[44] The method supplied a simple and powerful means of designing a complex pattern in the optical spectrum—by adding multiple waveforms together in a computer-controlled current program—and led us to the concept of etching spectral bar-codes in porous Si.

Construction of spectral bar-codes by Fourier synthesis

Berger's algorithm relies on a fundamental relationship between the spatial variation of refractive index in a material and the spectrum that it produces: the optical transform. The diffraction pattern generated when a laser beam impinges on a two-dimensional grating is a simple example of an optical transform.[45] Light passing through the diffraction grating generates a spot pattern that can be thought of as the two-dimensional Fourier-transform of the grating. Similarly, the optical spectrum that is obtained from a porous Si multilayer represents the Fourier transform of the porosity modulation in the film. Thus the spectrum that gives rise to the intense red, green, or blue color of the films shown in Fig. 3 consists of a single peak, at a frequency proportional to the frequency of the sine wave that the electrochemical apparatus applied while etching the film. Bovard *et al.* was the first to provide a theoretical analysis of how a Fourier transform could be used to design optical filters this way.[46]

The waveform superposition method we have used in preparing porous Si films is illustrated in Fig. 4.[47] First, several sine waves of different frequencies are generated and added together by computer (Fig. 4A). A single-crystal Si wafer is then etched with this composite current–time waveform (Fig 4B). The resulting porous Si film displays a porosity depth profile that maps directly to the current–time profile

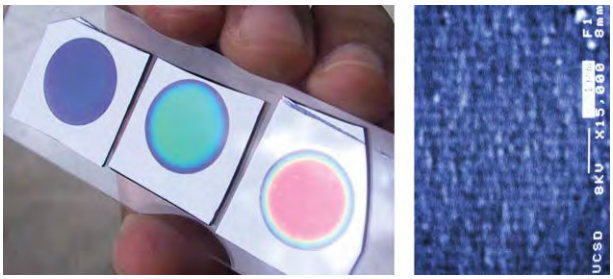

Fig. 3 Porous Si photonic crystals as inorganic analogues of the beetle shell. Left: Photograph of three one-dimensional photonic crystals made from porous Si. Right: Electron micrograph image showing the layered porous structure in a film. These samples are rugated structures, prepared by application of a sinusoidal current during etching. The different colors are produced using sine waves of different frequencies.

used in the etch (Fig. 4C). This porosity modulation is also a refractive index modulation, and each of the main peaks in the reflectivity spectrum of the sample (Fig. 4D) corresponds to one of the original sine waves used in designing the waveform (Fig. 4A). Thus the reflectivity spectrum (Fig. 4D) can be thought of as the Fourier transform of the composite current–time waveform (Fig. 4B) used in preparing the sample. Both the wavelength and the amplitude of the spectral peaks are controlled by the etching waveform, and each contains encoding information. The total possible number of codes that we have postulated is 4^{10}, or 1 048 576, based on demonstrated tunability of these two parameters.[47]

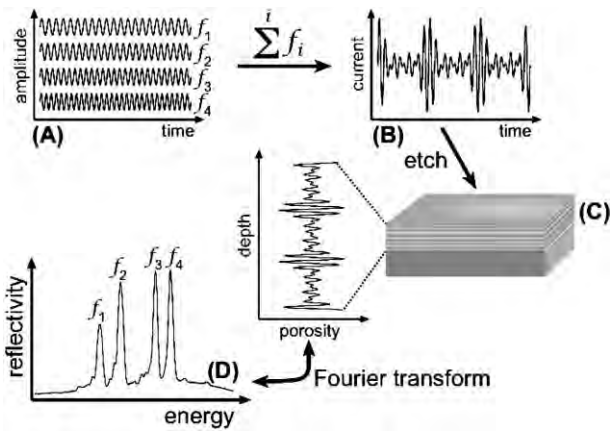

Fig. 4 Using the waveform superposition method to design a spectral code. In this example, four sine waves with different frequencies (A) are added together to generate a composite waveform that is then converted into a current–time waveform by the computer-controlled current source (B), etching a porosity-depth profile into the Si wafer (C). Representing the Fourier transform of the composite waveform, the resulting optical reflectivity spectrum (D) displays the four frequency components of the original four sine waves as separate spectral peaks. The position and intensity of each peak in the spectrum is determined by the frequency and amplitude, respectively, of its corresponding sine component.

Published on 10 February 2005. Downloaded by Open University on 07/07/2013 20:44:05.

The glass bead game

The photonic ID tag provides a rudimentary ability to probe the particle from a distance. Although not as robust as a radio transmitter, the photonic signature can be identified by a remote observer—distances up to 20 m have been demonstrated using a scanning laser system.[30] There are currently a variety of applications in which small particles must be identified at distances ranging anywhere from a few cm to several km. Much of the interest stems from the desire to construct large libraries of distinguishable beads onto which chemical reactions can be performed in a high-throughput fashion.[48] Bead-based systems can be used to screen for new drugs, identify specific genetic markers, and study genomic variation, for instance.[49,50] An extensive library of codes allows for parallel assays and more rapid screening techniques. Various schemes to incorporate identification codes have been proposed, involving either fluorescent molecules,[51] molecules with specific vibrational signatures,[52,53] quantum dots[54] or discrete metallic layers[55] as the encoding elements. The layered porous Si photonic structures offer some advantages over these other encoding methodologies. Porous silicon photonic crystals can be constructed that display features spanning the visible, NIR and IR region of the spectrum.[42] No other single material can support codes that span such a broad wavelength range. The reflectance spectra of photonic crystals can exhibit much sharper spectral features than can be obtained from a Gaussian ensemble of quantum dots or from an organic fluorophore. Thus more codes can be placed in a narrower spectral window. Most systems based on fluorescence are also limited by photobleaching and by low fluorescence quantum yields. Since photonic crystals are reflective systems, they do not have either of these two problems. In addition, the ability to read photonic crystals at near-infrared, tissue-penetrating wavelengths makes them amenable to *in vivo* applications. Systems that require imaging optics to read the codes, such as stratified metallic nanorods, need highly tolerant and relatively expensive read-out systems.[55] Finally, because the spectral code is integrated throughout the porous nanostructure, it is not possible for part of the code in a photonic crystal to be lost or scrambled.

Encoded materials are widely used in medical, forensic and remote sensing applications. In some instances, the encoded tracer needs to be coupled to a separate sensing element, such as a fluorescence assay. A unique feature of the porous silicon materials is that the identification and sensing functions can be performed by the same optical structure.

Sensing using porous silicon

The challenge for the "sensing" aspect of smart dust is perhaps the most difficult. Although sensing can be defined broadly in terms of imaging, motion detection, measurement of physical parameters such as temperature or light intensity, and identification of various chemical or biological species, here we focus on chemical and biochemical detection. The problem can be stated: "how do we place the sensitivity, specificity, and fidelity of a laboratory-scale chemical analysis on a grain of sand?" This requires building a functional nanostructure that responds to molecules.

The first use of porous Si as a chemical sensor was demonstrated by Tobias *et al.* in the late 1980s.[11] That sensor used capacitance changes in a porous Si layer upon adsorption of chemical species as a transduction method. There are now many physical properties of porous Si that have been harnessed for sensor applications, including capacitance,[11,56] resistance,[57] photoluminescence[58] and optical reflectivity.[59] Of the several electrical and optical transduction modes available to porous Si films, optical methods are perhaps the most extensively developed and possibly the most robust. Detection of toxins,[16,17] volatile organic compounds,[12,14,15] polycyclic aromatic hydrocarbons (PAHs),[13] explosives,[18] DNA[4,9] and proteins have all been reported,[5–7] and detection limits as low as a few ppb have been demonstrated for some of these.[60]

Molecular recognition

Molecular sensing can be further broken down into a recognition event and a signal transduction event. Recognition occurs when some physical or chemical property of the target analyte interacts with the sensor. This is what provides specificity to a sensor. Most biosensors incorporate a biomolecule such as an antibody or a DNA strand to provide specificity. Although Nature builds perhaps the most discriminating molecules for this purpose, they tend to be fairly unstable and do not survive well in sensors that must endure long-term exposure in the body or the environment. For medical point-of-care and clinical applications this is not a problem, because the sensors needed are typically single-use and operate for short periods of time. For longer-term applications such as real-time water or air quality monitoring, other approaches to recognition are needed. Porous Si offers some unique properties that can provide additional means of discriminating molecules. For example, the pore diameters can be controlled in such a way to allow discrimination of biomolecules based on their size.[23,61] Because the pores have a high aspect ratio, the residence time of a molecule in the nanostructure can be tuned, providing discrimination analogous to the retention phenomenon used in gas and liquid chromatography.[19,62] Additionally, various chemicals of non-biological origin can be attached to the porous Si surface. Freshly-etched porous Si is terminated with Si–H species, and these relatively reactive moieties are convenient synthons for a variety of hydrosilylation, oxidation, and electroless deposition reactions. In some cases the chemicals incorporated at the surface can be as discriminating as a biomolecule (H_2 sensors based on Pd coatings are notable),[63] although in general they are less discriminating but more robust. The various surface chemistries that allow the incorporation of recognition elements are the subject of a recent review.[64]

The second key component of sensing, signal transduction, occurs when the recognition event produces a signal that is observable in the macroscopic world. We have already seen how the spectral properties of porous Si photonic crystals can be used as encoding elements to allow identification of the device. In the following sections we will see how these same

 This journal is © The Royal Society of Chemistry 2005

Published on 10 February 2005. Downloaded by Open University on 07/07/2013 20:44:05.

photonic phenomena can be harnessed to respond to an analyte recognition event—the signal transduction aspect.

Sensing using the passive optical properties of porous silicon films

The first chemical sensor that utilized the passive optical properties of porous Si involved Fabry–Pérot interference from a thin layer.[59] The sensing principle of the single-layer Fabry–Pérot films as well as the more complex photonic crystals to be discussed shortly is based on what is commonly called the optical thickness of the film. Optical thickness, also known as "effective optical thickness", is the product of the refractive index (n) and the thickness (L) of the film. The electrochemical parameters used in the synthesis control both of these parameters precisely and reproducibly: the current density usually controls porosity and hence n, and the length of time that the sample is etched determines L. A high quality Fabry–Pérot film made of porous Si has two planar and parallel interfaces, and displays high fidelity fringes in the reflectivity spectrum (Fig. 5). A spectral shift in these fringes occurs when the refractive index of the film changes—for example when a molecule is admitted into the pores—corresponding to a change in optical thickness.[4]

The interference fringes observed in the reflectivity spectrum of a Fabry–Pérot film (Fig. 5) correspond to constructive and destructive interference from light reflected at the air/porous Si and porous Si/crystalline Si interfaces.[65] Reflectivity maxima are located at wavelengths determined by the Fabry–Pérot relationship (eqn. 1), where m is the spectral order of the fringe at wavelength λ, and the quantity nL is the optical thickness introduced above.[65] The factor of two in eqn. 1 comes from the fact that the path of light in the film is twice the thickness of the film when reflectivity is measured at normal incidence (see the inset to Fig. 5).

$$m\lambda = 2nL \tag{1}$$

A convenient means of extracting the value of nL is from the Fourier transform of the reflectivity spectrum. The Fourier transform of a plot of reflected intensity *versus* frequency yields a single peak whose position is the quantity $2nL$ (Fig. 6). The refractive index, n, in eqn. 1 is a composite index comprising a porosity-weighted average of the refractive indices of Si and of the medium filling the pores.[5] The composite index is often derived from the refractive index of the individual constituents and the porosity of the porous Si film by application of the Bruggeman effective medium model.[66–68]

Concentrating an analyte using a nanostructure

A standard approach in detecting very low concentrations of analyte is to pre-concentrate the sample. Materials with high surface area can be expected to collect a large number of molecules per unit volume based solely on surface adsorption effects (*e.g.* Langmuir adsorption, *etc.*). Nanoscale pores possess an additional capability to concentrate a vapor, known as microcapillary condensation. Originally described by Lord Kelvin in 1871,[69] microcapillary condensation is the physical tendency for a vapor to condense in a nanometre-sized pore at temperatures well above the dew point. It becomes significant at analyte pressures near a few percent of the saturation vapor pressure.

The relationship is described by the Kelvin equation[70] (eqn. 2), which relates the pore radius to the relative vapor pressure at which condensation occurs:

$$r = -\frac{\gamma V}{RT \ln (P/P^{o})} \tag{2}$$

Where r is the pore radius, γ is the surface tension of the gas/liquid interface, V is the molar volume of the liquid, R is the gas constant, P^{o} is the vapor pressure of the liquid at temperature T, and P is the observed pressure of the vapor. The model assumes that the pores are fully wetted by the liquid. The smaller the pore radius, the lower the partial pressure at which condensation can occur at a given temperature.[71] Microcapillary condensation is a truly nanoscale phenomenon that provides an additional means of spontaneously concentrating volatile molecules. The extent of both monolayer adsorption and capillary condensation are

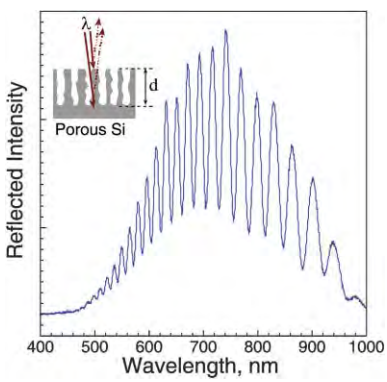

Fig. 5 Optical interference in a porous Si film. Reflectivity spectrum from a single layer porous Si film, showing the Fabry–Pérot interference phenomenon. A diagram showing the optical setup is shown in the inset.

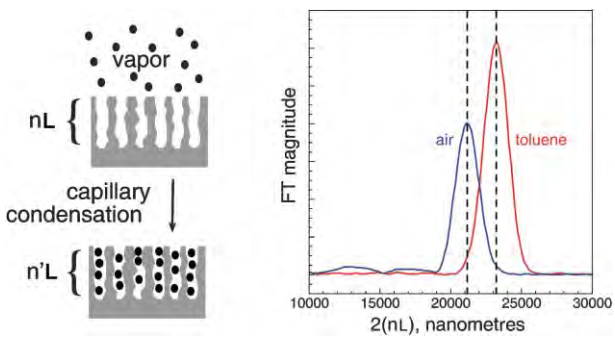

Fig. 6 Optical detection of molecules in a porous Si film. Fourier transform of the reflectivity spectra from a single-layer porous Si Fabry–Pérot film, showing the shift that occurs upon condensation of toluene into the pores. A diagram showing the experiment is given at the left. The pressure of toluene vapor detected here is 28 Torr.

Published on 10 February 2005. Downloaded by Open University on 07/07/2013 20:44:05.

influenced by the surface affinity of the porous matrix, which can be tailored by a range of chemical modifications.[20,72,73]

Signal processing with a nanostructure

Molecular electronics, involving the construction of digital circuits using molecules as the primary logic elements, is commonly promoted as the next wave in computer engineering.[74] Boolean logic concepts work well in the 100 nm to micron-sized world of digital electronics, but they may not transfer to data processing at the nanoscale. One could argue that Nature provides better examples of how to perform computation at the nanoscale, considering that Her devices have been operating successfully in this size regime for billions of years. Here we define computing to include signal processing, or the simplification, amplification, and/or translation of a stimulus. With the correct design, a nanomaterial can perform sophisticated mathematical transformations that greatly reduce the computational power needed to convert the stimulus into useable data. The replacement of a porous Si Fabry–Pérot film with a photonic crystal as a sensor element provides an example of a very simple mathematical operation, the Fourier transform, performed at the nanomaterials level.

Using a rugate filter to perform a Fourier transform

Earlier in this article we described how the Fourier transform of the spectrum of a Fabry–Pérot film can be used to measure chemical binding. A more sophisticated optical structure can yield this information directly, thus simplifying the analysis. Fig. 7 shows photographic images of small particles of porous Si prepared with a one-dimensional photonic crystal structure, known as a rugate filter. The particles are green in air and red in the presence of toluene vapor. Condensation of toluene in the nanopores has the same effect in the one-dimensional photonic crystal as it has in a Fabry–Pérot film, increasing the average refractive index of the nanostructure. However, the index change is easily visible by eye in the more sophisticated optical structure. The sinusoidal variation in index that comprises the rugate film leads to a single observable resonance that appears as a pure color to the eye, whereas the series of tightly-spaced fringes from the Fabry–Pérot layer of Fig. 5 cannot be resolved without the aid of a spectrometer. The Fourier transform performed at the materials level allows one to observe the effect of chemical binding directly.

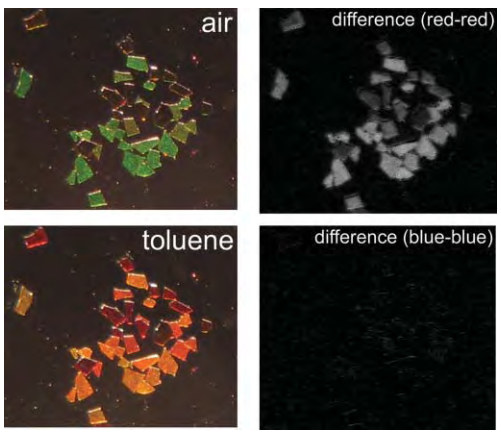

Fig. 7 Sensing volatile organic compounds (VOCs) using "smart dust" photonic crystals. An array of microscopic porous Si photonic crystals exposed to toluene vapor is shown in these images. The top left image is the collection held in air, bottom left is the sample after introduction of toluene vapor. When toluene condenses in the micropores, the refractive index of the entire particle increases, leading to a red shift in the photonic peak. The color change from green to red is easily observed with the naked eye. The images on the right are difference maps, showing the difference between the red (top right) and blue (bottom right) channels. The size of these particles is of the order of 300 μm, and their surfaces are modified with dodecyl functionalities. Images courtesy of Gordon M. Miskelly and Anne Ruminski

Optical structures more complicated than rugate films can be constructed that can provide added sensitivity or specificity for chemical sensing. Snow and coworkers[14] were the first to report vapor sensing with a Bragg stack, and Fauchet and coworkers demonstrated femtomolar-level detection of single-stranded DNA using a microcavity structure modified with a complementary-DNA fragment.[9,10] A lateral gradient of pore diameters can also be incorporated into such structures to provide size selectivity.[23,75]

Mobility

As devices become smaller, it becomes more difficult to locate them and to place them where you want them. Thus there is a need to develop tools to move and target nanostructures—what is referred to here as mobility. Three modes of mobility are of interest: autonomous motion, directed motion, and random motion. Autonomous motion, in which a nanostructure moves under its own power and follows a preprogrammed course without input from the user, is a grand challenge for nanotechnology. Although there are many examples from cellular biology, examples of autonomous motion of artificial nanostructures tend to be found only in the science fiction literature at present.[76–79] Directed motion is a little easier, and there are many examples of manipulation of nanostructures by an externally applied stimulus. Nanostructures have been manipulated by electrophoretic,[80–83] magnetic,[84–88] optical,[89] electrostatic[86,90] or mechanical[91] forces, and the tools of nanotechnology can even allow manipulation of individual atoms.[92] Random motion harnesses thermal fluctuations or Brownian effects[93] to move things about, and it would be limited were it not for the existence of the molecular forces that allow self-assembly. Self-assembly is one of the more celebrated tools used in the construction of nanostructures,[94] and it can also be used for their manipulation.

Self-assembling smart dust

In 2003 we developed a method to construct small particles of porous Si photonic crystals that could spontaneously self-assemble and orient at an interface.[31] The particles are prepared as platelets, with different chemistries on each side. If one side is hydrophobic and one side is hydrophilic, the chemically asymmetric particles will target an organic liquid/water interface, Fig. 8.

 This journal is © The Royal Society of Chemistry 2005

Published on 10 February 2005. Downloaded by Open University on 07/07/2013 20:44:05.

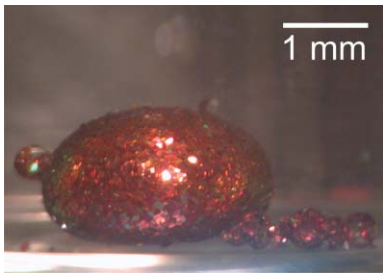

Fig. 8 Amphiphilic "smart dust" particles self-assembled at an oil/water interface. The microscopic particles consist of two stacked rugate structures, one green and the other red. Each side is chemically modified to have different surface affinities. The chemically asymmetric particles spontaneously target and align themselves at an organic liquid/water interface with the hydrophobic (green) side oriented toward the organic phase and the hydrophilic (red) side toward the water.

The technique for synthesizing these chemically asymmetric nanostructures involves five steps, outlined in Fig. 9. In the first step, a photonic crystal is etched. The second step involves chemically modifying the porous silicon photonic structure so that it will find and stick to the desired target. In the present case, we target the interface between a drop of oil and water, so the targeting chemistry employs a hydrophobic molecule. The hydrosilylation reaction mentioned earlier is convenient, because it attaches the molecule to the porous Si *via* a Si–C bond.[64] Si–C bound species are robust enough to survive a subsequent electrochemical etch, which places a second photonic crystal directly beneath the first one. A current pulse releases the entire porous structure from the substrate, and ultrasonication pulverizes it into small particles. A subsequent reaction can then be performed on the second side. A chemical oxidation is performed in the present example. It will be seen that this platform methodology can be used to construct elaborate structures with a variety of useful optical and mechanical properties.

Once added to an oil–water mixture, the particles orient, or "tile" themselves on the interface. In this way the particles behave like a lipid or surfactant molecule, targeting with the hydrophobic side oriented toward the organic phase and the hydrophilic side toward the water. As a means of signaling their presence at the interface, the particles change color. As the nanostructure comes in contact with the oil drop, some of the liquid is drawn in. The hydrophobic liquid only wicks into the regions of the nanostructure that have been modified with the hydrophobic chemistry. The refractive index of the liquid in the nanostructure causes a predictable shift in the spectrum, signaling to the outside observer that the target has been located.

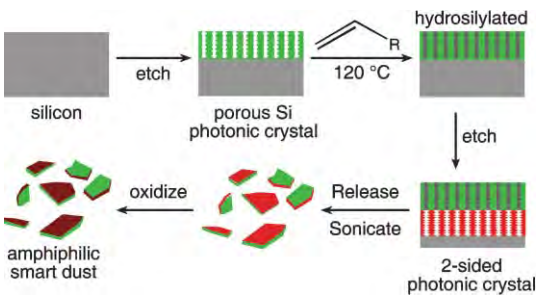

Fig. 9 Synthesis of self-assembling smart dust involves sequential electrochemical etching and chemical modification steps.

Directing motion with magnetic smart dust

The synthetic scheme described in Fig. 9 can be used to add magnetic properties to smart dust.[95] Porous Si microparticles are exposed to superparamagnetic nanoparticles of Fe_3O_4 in the last step of Fig. 9, and the magnetic nanoparticles become attached as the layer oxidizes. The particles adhere to microlitre-scale liquid droplets, allowing the droplets to be manipulated with a permanent magnet or an electromagnet (Fig. 10). The reflectivity spectrum from the amphiphilic photonic crystals provides a signal that can be used to identify the payload. We have demonstrated a simple precipitation reaction by bringing a drop of water containing silver ions into contact with one containing iodide, but the concept should be generally applicable to a variety of chemical reactions and bioassays, including transformations involving single cells. Such controlled manipulation of small volumes is a challenging problem in microfluidics,[86,96–98] and it is a key requirement for many high-throughput analyses, syntheses, and microassays.[99,100]

Conclusions

The challenge for the nanotechnology community addressed in this article involves engineering the functional complexity of a macroscopic machine into something the size of a grain of sand. This article has focused on passive devices with very limited capabilities compared with those of an integrated circuit chip. Pister's "autonomous sensing, computing, and communication system" that is "packed into … a small particle or speck" provided the inspiration. The translation of his microscale concepts to the nanoscale has been realized in a

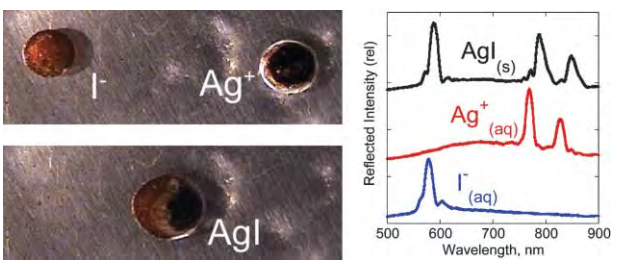

Fig. 10 Smart dust chaperones for chemical reactants. Encoded magnetic "smart dust" particles self-assembled on two drops of water (top left). The microscopic particles are photonic crystals of porous silicon that spontaneously assemble at the surface of the water drops. A magnetic field has been applied to bring the two drops together (bottom left), resulting in a reaction between the chemicals contained in the two drops (silver ions in one, iodide ions in the other). The silver iodide precipitate that forms in the reaction is evident as a whitish cloud inside the drop. The reflectivity spectra of the particles (right) indicate the identity of each drop before reaction and of the combination after reaction. The smaller drops each contain 3 μmol of reagent, the volume of each drop is 30 μl.

Published on 10 February 2005. Downloaded by Open University on 07/07/2013 20:44:05.

very rudimentary fashion, but advances that allow us to incorporate the complex processing capability of active circuits into a nanoscale device are still needed. Although it becomes more difficult to engineer functional complexity as the device shrinks, there are compelling reasons to make dust-sized machines, particularly in the field of medicine. Teaching smart dust to move under its own power, respond to a stimulus, and deliver a payload at a predetermined time and place are the next challenges.

Acknowledgements

The authors thank Prof. Kristofer Pister of the University of California, Berkeley, Prof. Sangeeta N. Bhatia, Jason R. Dorvee, Yang Yang Li, Chae-Yoon Lim, Kenneth MacGillivray, Shawn O. Meade, Claudia Pacholski, and Anne Ruminski of the University of California, San Diego, and especially Gordon M. Miskelly of the University of Auckland, New Zealand, for helpful discussions. The authors thank Prof. Andrew Parker, of the Oxford University Zoology Department and Company of Biologists, Ltd., for permission to reproduce photographs of the beetle shell used in Fig. 2. The projects described in this article have been funded in part with Federal funds from the Air Force Office of Scientific Research under Grant No. F49620-02-1-0288, the National Science Foundation Division of Materials Research, the US EPA STAR program (Grant #R829619) and the National Cancer Institute, National Institutes of Health, Contract No. N01-CO-37117. JRL thanks the UCSD California Institute of Telecommunications and Information Technology for a graduate fellowship.

Michael J. Sailor and Jamie R. Link
Department of Chemistry and Biochemistry, University of California, San Diego, 9500 Gilman Drive, m/c 0358, La Jolla, CA 92093-0358, USA. E-mail: msailor@ucsd.edu; Fax: +1 858 534 5383; Tel: +1 858 534 8188

References

1 B. Warneke, M. Last, B. Liebowitz and K. S. J. Pister, *Computer*, 2001, **34**, 44.
2 I. F. Akyildiz, W. Su, Y. Sankarasubramaniam and E. Cayirci, *Comput. Networks*, 2002, **38**, 393.
3 K. S. Yun, J. Gil, J. Kim, H. J. Kim, K. Kim, D. Park, M. S. Kim, H. Shin, K. Lee, J. Kwak and E. Yoon, *Sens. Actuators B*, 2004, **102**, 27.
4 V. S.-Y. Lin, K. Motesharei, K. S. Dancil, M. J. Sailor and M. R. Ghadiri, *Science*, 1997, **278**, 840.
5 A. Janshoff, K.-P. S. Dancil, C. Steinem, D. P. Greiner, V. S.-Y. Lin, C. Gurtner, K. Motesharei, M. J. Sailor and M. R. Ghadiri, *J. Am. Chem. Soc.*, 1998, **120**, 12108.
6 S. Zangooie, R. Bjorklund and H. Arwin, *Thin Solid Films*, 1998, **313–314**, 825.
7 K.-P. S. Dancil, D. P. Greiner and M. J. Sailor, *J. Am. Chem. Soc.*, 1999, **121**, 7925.
8 D. van Noort, S. Welin-Klintstrom, H. Arwin, S. Zangooie, I. Lundstrom and C.-F. Mandenius, *Biosens. Bioelectron.*, 1998, **13**, 439.
9 S. Chan, P. M. Fauchet, Y. Li, L. J. Rothberg and B. L. Miller, *Phys. Status Solidi A*, 2000, **182**, 541.
10 S. Chan, S. R. Horner, B. L. Miller and P. M. Fauchet, *J. Am. Chem. Soc.*, 2001, **123**, 11797.
11 R. C. Anderson, R. S. Muller and C. W. Tobias, *Sens. Actuators*, 1990, **A21-A23**, 835.
12 J. M. Lauerhaas, G. M. Credo, J. L. Heinrich and M. J. Sailor, *J. Am. Chem. Soc.*, 1992, **114**, 1911.
13 J. H. Song and M. J. Sailor, *J. Am. Chem. Soc.*, 1997, **119**, 7381.
14 P. A. Snow, E. K. Squire, P. S. J. Russell and L. T. Canham, *J. Appl. Phys.*, 1999, **86**, 1781.
15 S. Zangooie, R. Jansson and H. Arwin, *J. Appl. Phys.*, 1999, **86**, 850.
16 S. Létant and M. J. Sailor, *Adv. Mater.*, 2000, **12**, 355.
17 H. Sohn, S. Létant, M. J. Sailor and W. C. Trogler, *J. Am. Chem. Soc.*, 2000, **122**, 5399.
18 S. Content, W. C. Trogler and M. J. Sailor, *Chem. Eur. J.*, 2000, **6**, 2205.
19 P. Allcock and P. A. Snow, *J. Appl. Phys.*, 2001, **90**, 5052.
20 J. Gao, T. Gao, Y. Li and M. J. Sailor, *Langmuir*, 2002, **18**, 2229.
21 L. T. Canham, M. P. Stewart, J. M. Buriak, C. L. Reeves, M. Anderson, E. K. Squire, P. Allcock and P. A. Snow, *Phys. Status Solidi A*, 2000, **182**, 521.
22 Y. Y. Li, F. Cunin, J. R. Link, T. Gao, R. E. Betts, S. H. Reiver, V. Chin, S. N. Bhatia and M. J. Sailor, *Science*, 2003, **299**, 2045.
23 B. E. Collins, K.-P. Dancil, G. Abbi and M. J. Sailor, *Adv. Funct. Mater.*, 2002, **12**, 187.
24 F. V. Mikulec, J. D. Kirtland and M. J. Sailor, *Adv. Mater.*, 2002, **14**, 38.
25 H. Presting, J. Konle, V. Starkov, A. Vyatkin and U. Konig, *Mater. Sci. Eng., B*, 2004, **108**, 162.
26 T. Pichonat, B. Gauthier-Manuel and D. Hauden, *Chem. Eng. J.*, 2004, **101**, 107.
27 S. Gold, K. L. Chu, C. Lu, M. A. Shannon and R. I. Masel, *J. Power Sources*, 2004, **135**, 198.
28 V. Chin, B. E. Collins, M. J. Sailor and S. N. Bhatia, *Adv. Mater.*, 2001, **13**, 1877.
29 J. L. Heinrich, C. L. Curtis, G. M. Credo, K. L. Kavanagh and M. J. Sailor, *Science*, 1992, **255**, 66.
30 T. A. Schmedake, F. Cunin, J. R. Link and M. J. Sailor, *Adv. Mater.*, 2002, **14**, 1270.
31 J. R. Link and M. J. Sailor, *Proc. Natl. Acad. Sci. USA*, 2003, **100**, 10607.
32 N. Hall, *Chem. Commun.*, 2003, **21**, 2639.
33 A. R. Parker, D. R. Mckenzie and M. C. J. Large, *J. Exp. Biol.*, 1998, **201**, 1307.
34 G. Vincent, *Appl. Phys. Lett.*, 1994, **64**, 2367.
35 E. Yablonovitch, *Phys. Rev. Lett.*, 1987, **58**, 2059.
36 S. John, *Phys. Rev. Lett.*, 1987, **58**, 2486.
37 M. Cazzanelli, C. Vinegoni and L. Pavesi, *J. Appl. Phys.*, 1999, **85**, 1760.
38 V. Lehmann, R. Stengl, H. Reisinger, R. Detemple and W. Theiss, *Appl. Phys. Lett.*, 2001, **78**, 589.
39 C. Mazzoleni and L. Pavesi, *Appl. Phys. Lett.*, 1995, **67**, 2983.
40 L. Pavesi and P. Dubos, *Semicond. Sci. Technol.*, 1997, **12**, 570.
41 V. Pellegrini, A. Tredicucci, C. Mazzoleni and L. Pavesi, *Phys. Rev. B*, 1995, **52**, R14328.
42 M. Thönissen and M. G. Berger, Multilayer structures of porous silicon, in *Properties of Porous Silicon*, vol. 18, ed. L. Canham, Short Run Press Ltd, London, 1997, p. 30.
43 S. Zangooie, M. Schubert, C. Trimble, D. W. Thompson and J. A. Woollam, *Appl. Opt.*, 2001, **40**, 906.
44 M. G. Berger, R. Arens-Fischer, M. Thoenissen, M. Krueger, S. Billat, H. Lueth, S. Hilbrich, W. Theiss and P. Grosse, *Thin Solid Films*, 1997, **297**, 237.
45 A. B. Ellis, M. J. Geselbracht, B. J. Johnson, G. Lisensky and W. R. Robinson, *Teaching general chemistry: A materials science companion'*, American Chemical Society, Washington, DC, 1993.
46 B. G. Bovard, *Appl. Opt.*, 1993, **32**, 5427.
47 S. O. Meade, M. S. Yoon, K. H. Ahn and M. J. Sailor, *Adv. Mater.*, 2004, **16**, 1811.
48 J. A. Ferguson, T. C. Boles, C. P. Adams and D. R. Walt, *Nat. Biotechnol.*, 1996, **14**, 1681.
49 K. Braeckmans, S. C. D. Smedt, M. Leblans, R. Pauwels and J. Demeester, *Nat. Rev. Drug Discovery*, 2002, **1**, 447.
50 W. C. Still, *Acc. Chem. Res.*, 1996, **29**, 155.
51 J. R. Epstein, A. P. K. Leung, K.-H. Lee and D. R. Walt, *Biosens. Bioelectron.*, 2003, **18**, 541.
52 H. Fenniri, L. Ding, A. E. Ribbe and Y. Zyrianov, *J. Am. Chem. Soc.*, 2001, **123**, 8151.

 This journal is © The Royal Society of Chemistry 2005

Published on 10 February 2005. Downloaded by Open University on 07/07/2013 20:44:05.

53 H. Fenniri, H. G. Hedderich, K. S. Haber, J. Achkar, B. Taylor and D. Ben-Amotz, *Angew. Chem., Int. Ed.*, 2000, **39**, 4483.
54 W. C. W. Chan and S. Nie, *Science*, 1998, **281**, 2016.
55 S. R. Nicewarner-Peña, R. G. Freeman, B. D. Reiss, L. He, D. J. Peña, I. D. Walton, R. Cromer, C. D. Keating and M. J. Natan, *Science*, 2001, **294**, 137.
56 Z. M. Rittersma, A. Splinter, A. Bodecker and W. Benecke, *Sens. Actuators, B*, 2000, **B68**, 210.
57 M. Ben-Chorin, A. Kux and I. Schechter, *Appl. Phys. Lett.*, 1994, **64**, 481.
58 J. M. Lauerhaas and M. J. Sailor, *Science*, 1993, **261**, 1567.
59 C. L. Curtis, V. V. Doan, G. M. Credo and M. J. Sailor, *J. Electrochem. Soc.*, 1993, **140**, 3492.
60 M. Thönissen and M. G. Berger, Sensor applications of porous silicon, in *Properties of Porous Silicon*, vol. 18, ed. L. Canham, Short Run Press Ltd, London, 1997, p. 364.
61 L. M. Karlsson, M. Schubert, N. Ashkenov and H. Arwin, *Thin Solid Films*, 2004, **455–456**, 726–730.
62 S. Létant and M. J. Sailor, *Adv. Mat.*, 2001, **13**, 335.
63 H. Lin, T. Gao, J. Fantini and M. J. Sailor, *Langmuir*, 2004, **20**, 5104.
64 J. M. Buriak, *Chem. Rev.*, 2002, **102**, 1272.
65 E. Hecht, *Optics*, Addison-Wesley, Reading, MA, 1998.
66 C. F. Bohren and D. R. Huffman, *Adsorption and scattering of light by small particles*, Wiley, New York, 1983.
67 C. Pickering, M. I. J. Beale, D. J. Robbins, P. J. Pearson and R. F. Greef, *Thin Solid Films*, 1985, **125**, 157.
68 C. Pickering, M. I. J. Beala, D. J. Robbins, P. J. Pearson and R. Greef, *J. Phys. C: Solid State Phys.*, 1984, **17**, 6535.
69 W. Thomson, *Philos. Mag.*, 1871, **42**, 448.
70 J. N. Israelachvili, *Intermolecular and surface forces*, Academic Press, London, 1992.
71 A. W. Adamson, *Physical Chemistry of Surfaces*, John Wiley & Sons, Inc., New York, 1990.
72 J. Gao, T. Gao and M. J. Sailor, *Appl. Phys. Lett.*, 2000, **77**, 901.
73 T. Gao, J. Gao and M. J. Sailor, *Langmuir*, 2002, **18**, 9953.
74 A. Aviram and M. Ratner, in Molecular electronics : Science and technology, in *Ann. NY Acad. Sci.*, vol. 852, New York Academy of Sciences, New York, 1998.
75 Y. Y. Li, P. Kim and M. J. Sailor, *Phys. Status Solidi A*, 2005, in press.
76 D. Seuss, *The Cat in the Hat Comes Back!*, Beginner Books: Distributed by Random House, 1958.
77 I. Asimov, H. Kleiner and O. Klement, *Fantastic Voyage*, Houghton Mifflin, 1966.
78 N. Stephenson, *Diamond age, or, a young lady's illustrated primer*, Bantam Books, 1995.
79 M. Crichton, *Prey*, Harper Collins, 2002.
80 C. F. Edman, R. B. Swint, C. Gurtner, R. E. Formosa, S. D. Roh, K. E. Lee, P. D. Swanson, D. E. Ackley, J. J. Coleman and M. J. Heller, *IEEE Photon. Technol. Lett.*, 2000, **12**, 1198.
81 A. Eychmüller, L. Katsikas and H. Weller, *Langmuir*, 1990, **6**, 1605.
82 H. K. Jones and N. E. Ballou, *Anal. Chem.*, 1990, **62**, 2484.
83 G. H. Markx, R. Pethig and J. Rousselet, *J. Phys. D*, 1997, **30**, 2470.
84 C. Haber and D. Wirtz, *Rev. Sci. Instrum.*, 2000, **71**, 4561.
85 J. N. Anker, C. Behrend and R. Kopelman, *J. Appl. Phys.*, 2003, **93**, 6698.
86 P. Aussillous and D. Quere, *Nature*, 2001, **411**, 924.
87 A. Ito, Y. Takizawa, H. Honda, K.-I. Hata, H. Kagami, M. Ueda and T. Kobayashi, *Tissue Eng.*, 2004, **10**, 833.
88 E. Mirowski, J. Moreland, S. E. Russek and M. J. Donahue, *Appl. Phys. Lett.*, 2004, **84**, 1786.
89 A. Ashkin, J. M. Dziedzic, J. E. Bjorkholm and S. Chu, *Opt. Lett.*, 1986, **11**, 288.
90 S. Tsonchev, G. C. Schatz and M. A. Ratner, *J. Phys. Chem. B*, 2004, **108**, 8817.
91 D. S. Ginger, H. Zhang and C. A. Mirkin, *Angew. Chem., Int. Ed.*, 2004, **43**, 30.
92 M. F. Crommie, C. P. Lutz and D. M. Eigler, *Science*, 1993, **262**, 218.
93 C. J. Behrend, J. N. Anker and R. Kopelman, *Appl. Phys. Lett.*, 2004, **84**, 154.
94 Y. Xia, J. A. Rogers, K. E. Paul and G. M. Whitesides, *Chem. Rev.*, 1999, **99**, 1823.
95 J. R. Dorvee, A. M. Derfus, S. N. Bhatia and M. J. Sailor, *Nat. Mater.*, 2004, **3**, 896.
96 O. D. Velev, B. G. Prevo and K. H. Bhatt, *Nature*, 2003, **426**, 515.
97 B. Zheng, J. D. Tice, L. S. Roach and R. F. Ismagilov, *Angew. Chem., Int. Ed.*, 2004, **43**, 2508.
98 V. Srinivasan, V. K. Pamula and R. B. Fair, *Anal. Chim. Acta*, 2004, **507**, 145.
99 J. Liu, C. Hansen and S. R. Quake, *Anal. Chem.*, 2003, **75**, 4718.
100 J. W. Hong and S. R. Quake, *Nat. Biotechnol.*, 2003, **21**, 1179.